

Zeolite 4A filled poly (3, 4-ethylenedioxythiophene): (polystyrenesulfonate) (PEDOT: PSS) and polyvinyl alcohol (PVA) blend nanocomposites as high-k dielectric materials for embedded capacitor applications

M. K. Mohanapriya¹, Kalim Deshmukh², M. Basheer Ahamed², K. Chidambaram¹, S. K. Khadheer Pasha^{1*}

¹Department of Physics, School of Advanced Sciences, VIT University, Vellore 632014, Tamilnadu, India

²Department of Physics, B. S. Abdur Rahman University, Chennai 600048, Tamilnadu, India

*Corresponding author. Tel: (+91) 9894665388; E-mail: skkhadheerpasha@vit.ac.in

Received: 20 March 2016, Revised: 06 May 2016 and Accepted: 20 June 2016

ABSTRACT

Zeolite 4A nanoparticles were incorporated into Poly (3, 4 - ethylenedioxythiophene): poly (styrenesulfonate) (PEDOT: PSS) and Polyvinyl alcohol (PVA) blend matrix to prepare PEDOT: PSS/PVA/Zeolite 4A nanocomposites using solution casting technique. The structure and morphology of nanocomposites were examined using Fourier transform infrared spectroscopy, X-ray diffraction, UV-Vis spectroscopy and Scanning electron microscopy. The mechanical and dielectric properties of nanocomposites were also evaluated. The FTIR and XRD results indicate the strong interaction between the Zeolite 4A nanoparticles and the polymer matrix. The SEM micrographs show the homogeneous dispersion of Zeolite 4A into the polymer matrix. The nanocomposite exhibits a high dielectric constant and low dielectric loss, which could be due to proper dispersion and good interaction between Zeolite 4 A and polymer matrix. Thus, based on the results obtained it can be concluded that PEDOT: PSS/PVA/Zeolite 4A nanocomposites can be used as a flexible dielectric material for embedded capacitor applications. Copyright © 2016 VBRI Press.

Keywords: Zeolite 4A; PEDOT: PSS; dielectric properties; SEM.

Introduction

Over the last two decades, applications of polymer-inorganic nanocomposites have seen incredible growth in many fields. The addition of inorganic nanoparticles to polymers allows the implementation of new features in the polymer matrix by modifying their physical properties [1-3]. Polymer nanocomposites have unique properties such as light weight, high flexibility and low cost. The optical and electrical properties of polymers can be improved to a great extent by using suitable nanofiller with controlled loading [4]. Polymer nanocomposite combines the advantages of individual material; for example, the flexibility and processability of polymers, and the selectivity and thermal stability of the inorganic fillers. Two types of inorganic particles can be used as fillers in polymers for preparing composite materials, i.e., porous and nonporous. Various types of porous inorganic fillers such as zeolites and carbon molecular sieves have been used for mixed matrix nanocomposites for membrane applications and investigated for their effect on structural and gas separation properties [5, 6]. Inorganic nonporous nanoparticles have also been introduced into the polymer matrix to prepare polymer-inorganic nanocomposite

[7-10]. The formation of nanocomposite with more than two components is used to achieve superior properties of their constituents. Because of the presence of more than one component in the nanocomposites, the properties of nanocomposites are subjected to many factors such as filler content, filler property and interfacial adhesion [7, 11]. To improve the interaction between the filler with the polymer matrix and adhesion properties of the filler a crosslinking compound is added to the polymer matrix.

Poly (3, 4-ethylenedioxythiophene): poly (styrene sulfonate) (PEDOT: PSS) has attracted considerable attention because of its superior electrical conductivity, high thermal stability and excellent chemical and environmental stability. PEDOT: PSS is one of the most promising conducting polymers for various electronics and optoelectronic device applications [12, 13] because of its excellent transparency and film forming ability. It is commonly used as the anode electrode material in organic electronics such as field-effect transistors and photovoltaic cells [14]. PEDOT: PSS has also been used in many industrial applications such as solar cells [15], light emitting diodes (LEDs) [16, 17], in antistatic coatings [18, 19], electrochromic devices [20] and polymer photovoltaics [21]. Owing to these merits, large numbers of

research groups are exploring the chemistry of PEDOT: PSS in order to improve its properties. One way of improving the properties of PEDOT: PSS is by introducing other polymers to form polymer blends or introducing nanofillers to form nanocomposites.

Poly (vinyl alcohol) (PVA) is a semi-crystalline, water soluble polymer that has been studied extensively because of its many desirable properties such as easy preparation, excellent chemical resistance, biocompatibility, biodegradability and low cost [22-24]. PVA is a synthetic polymer having excellent film-forming, emulsifying, and adhesive properties [25]. PVA is a well-known membrane material with good mechanical properties. Therefore, it has been used for membrane application [26] drug delivery systems [27] and artificial biomedical devices [28]. PVA is a good candidate for blending with PEDOT: PSS because of the presence of hydroxyl groups in the carbon backbone chain of PVA. The addition of PVA to PEDOT: PSS can enhance the flexibility and durability of the blend films [29]. In this study, PVA is blended with PEDOT: PSS which renders the formation of free-standing films.

Zeolites are crystalline aluminosilicate of group IA and group IIA elements, such as sodium, potassium, magnesium and calcium [30, 31]. Zeolites have a rigid, three-dimensional crystalline frameworks arising from an open framework of SiO_4 and AlO_4 linked together. Zeolites have some superior properties such as high ion-exchange and high adsorption capacity. It can absorb large quantities of vapor, such as water, ammonia and carbon oxides even at low partial pressures. These properties enable to use Zeolite in energy storage applications [32]. Zeolites are also used in the industry and they have many applications in the field of wastewater treatment and gas separation [33]. Zeolites are the attractive native material for removing heavy metal ions from industry and processing effluent water because it has advantages such as high abrasion resistance and low swelling capacity [34]. Zeolites are the most favorable nanofillers for polymers due to the highly ordered porous structure with very small pore size. Zeolites 4A have three-dimensional pore structure and these pores are composed of four-membered rings. Due to its low cost and high thermal stability, Zeolite 4A has potential applications in catalysis processes [35, 36].

Table 1. Feed compositions of PEDOT: PSS/PVA/Zeolite 4A nanocomposites.

PEDOT: PSS (wt %)	PVA (wt %)	Zeolite 4A (wt %)
50	50	0
25	70	5
20	70	10
15	70	15
10	70	20

In the present work, Zeolite 4 A with different concentrations has been used as nanofiller for PEDOT: PSS/PVA blend matrix. PEDOT: PSS/PVA/Zeolite 4A nanocomposites were prepared using simple and eco-friendly solution casting technique. The nanocomposites were characterized using different analytical techniques including FTIR, XRD, UV-Vis, SEM and tensile test. The main purpose of this study is to have a deeper insight into

fundamental characterizations and the dielectric behavior of PEDOT: PSS/PVA blend films reinforced with different concentrations of Zeolite 4A nanoparticles.

Experimental

Materials and methods

PVA of molecular weight 78,000 g/mol was purchased from Merck Schuchart, Germany. The aqueous dispersion of PEDOT: PSS was purchased from Sigma Aldrich, India. Zeolite 4A used in present study was purchased from Advanced Specialty Gas Equipment ASGE, USA. Ultra-pure Milli-Q water was used as solvent throughout the study.

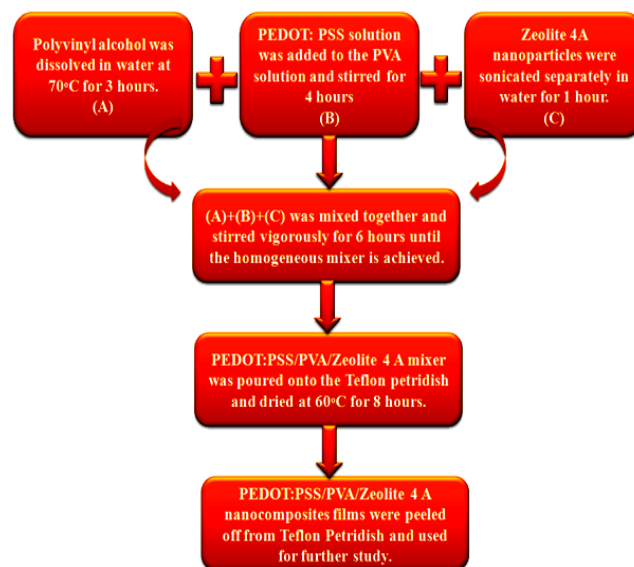


Fig. 1. Protocol for the synthesis of PEDOT: PSS/PVA/Zeolite 4A nanocomposites.

Synthesis of PEDOT: PSS/PVA/Zeolite 4A nanocomposites

PEDOT: PSS/PVA/Zeolite4A nanocomposite films with different loadings (0, 5, 10, 15, 20 wt %) of Zeolite 4A particles were prepared by solution casting method. The feed compositions of nanocomposites are given in **Table 1**. Protocol for the synthesis of PEDOT: PSS/PVA/Zeolite4A nanocomposite is given in **Fig. 1**. In a typical synthesis process, PVA was first dissolved appropriately in distilled water at 70 °C for 3 hours. The PVA aqueous solution was kept aside until it's cool down. Later, a known quantity of PEDOT: PSS solution was added to PVA solution and continuously stirred for 4 hours. On the other hand, the Zeolite 4A powder was sonicated separately in water for one hour and subsequently mixed with PEDOT: PSS/PVA solution. The PEDOT: PSS/PVA/Zeolite4A dispersion was further stirred (500 rpm) at room temperature (30 °C) for 6 hours until the homogeneous dispersion is obtained. The resulting homogeneous dispersion of PEDOT: PSS/PVA/Zeolite4A was poured on to a Teflon Petridish and dried in a hot air oven at 60 °C for 8 hours. The PEDOT: PSS/PVA/Zeolite4A nanocomposite films of thickness in the range of 50-60 μm were peeled off from the Petridish and used for further studies.

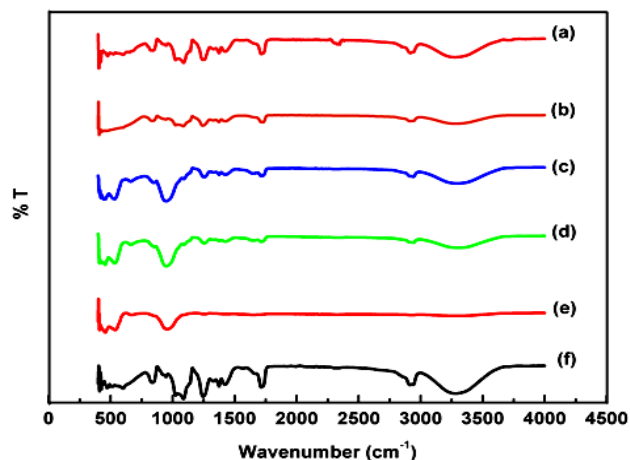


Fig. 2. FTIR spectra of PEDOT: PSS/PVA/Zeolite 4A nanocomposites films (a) neat PVA (b) PEDOT: PSS/PVA blend (c) 5 wt % Zeolite 4A (d) 10 wt % Zeolite 4A (e) 15 wt % Zeolite 4A (f) 20 wt % Zeolite 4A.

Characterizations

FTIR spectroscopy of PEDOT: PSS/PVA/Zeolite 4A nanocomposite film was carried out with Fourier transform infrared spectrophotometer (Shimadzu, IRAffinity-1, Japan) in the wave number range 400–4000 cm^{-1} in the transmittance mode.

X-ray diffraction patterns of PEDOT: PSS/PVA/Zeolite 4A nanocomposite films were recorded using Cu K α radiation of wavelength $\lambda = 1.54060 \text{ \AA}$ with a graphite monochromator produced by a Bruker AXS D8 focus advanced X-ray diffraction meter (Rigaku, Tokyo, Japan) with 'Ni-filtered'. The scans were taken in the 2θ range from 10° to 60° with a scanning speed and step size of $1^\circ/\text{min}$ and 0.01° , respectively. UV-vis absorption spectra of PEDOT: PSS/PVA/Zeolite 4A dispersion was obtained in the range of 190–600 nm with a Shimadzu UV-2401PC, UV-vis spectrophotometer. Surface morphology of the PEDOT: PSS/PVA/Zeolite 4A nanocomposite was examined by Hitachi Quanta 200 scanning electron microscope. Before taking the images, the samples were sputtered with gold in the vacuum evaporator. An accelerating voltage of 15 kV was applied to obtain the SEM images.

The tensile strength of PEDOT: PSS/PVA/Zeolite 4A nanocomposite film was studied using bench top tester (H50K-S UTM, maker: Tinius Olsen, Horsham, USA). The sample dimensions of $10 \times 20 \times 0.05 \text{ mm}$ were used for mechanical test.

The dielectric properties of PEDOT: PSS/PVA/Zeolite 4A nanocomposite films were measured using Wayne Kerr 6500B Precision Impedance Analyzer (Chichester, West Sussex, UK), in the broad band frequency ranging from 50 Hz to 20 MHz and temperature ranging from 40 – 150°C .

Results and discussion

FTIR spectroscopy

The FTIR spectroscopy is one of the most favorable techniques to study the interaction between the molecules and the functional groups present in the nanocomposites. The FTIR spectra of neat PVA and PEDOT: PSS/PVA

blend were shown in **Fig. 2(a, b)**. The FTIR spectrum of PVA shows various characteristic peaks at 916 and 840 cm^{-1} which are attributed to skeletal vibration of PVA [22, 37]. The characteristic band at 3286 and 1084 cm^{-1} are due to O–H stretching and C–O stretching vibrations, respectively. The band at 2928 cm^{-1} corresponds to C–H asymmetric stretching vibration of the alkyl group and the band at 1724 cm^{-1} is attributed to the C=O stretching vibration of the carbonyl group. Also, the band at 1655 cm^{-1} can be assigned to an acetyl C=O group of PVA. The band at 1084 cm^{-1} corresponds to the C–O stretching vibration of an acetyl group. The band at 1321 cm^{-1} and 1243 cm^{-1} are attributed to CH_2 and C–H wagging vibrations respectively. The band at 1438 cm^{-1} corresponds to CH_2 bending [22, 23]. The FTIR spectra of PEDOT: PSS/PVA blend (**Fig. 2 (b)**) shows small shifts in the bands as compare to the neat PVA film. This indicates the considerable interactions between two polymers. The FTIR spectra of PEDOT: PSS/PVA/Zeolite 4A nanocomposite with different loading percentage of zeolite 4A is shown in **Fig. 2 (c–f)**. The characteristic peaks of Zeolite 4A at 957 cm^{-1} and 1250 cm^{-1} corresponding to Si–O–Si and Si–O–Al stretching vibration were observed in the FTIR spectra of nanocomposite [38]. A significant change in the intensity and shifts of bands were observed in the FTIR spectroscopy results of nanocomposites which indicate significant interaction between the constituents of nanocomposites.

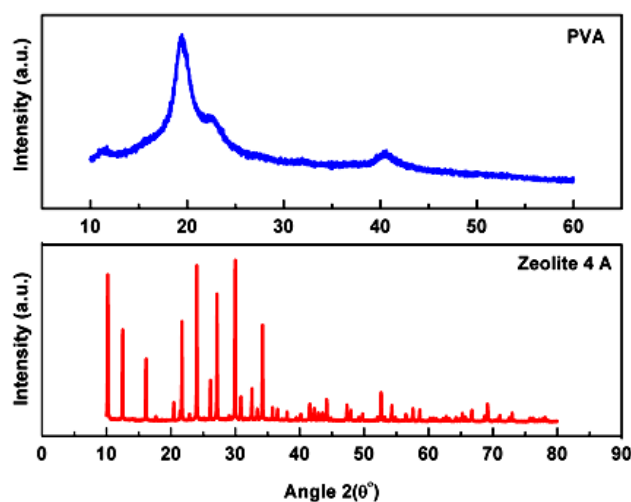


Fig. 3. XRD spectra of PVA and Zeolite 4A nanoparticles.

X-ray diffraction

The X-ray diffraction patterns of PEDOT: PSS/PVA/Zeolite 4A nanocomposites were obtained to understand the structural change in the PEDOT: PSS/PVA blend matrix upon addition of Zeolite 4A. **Fig. 3** shows the XRD pattern of neat PVA and Zeolite 4A nanoparticles. Since PVA is a semi-crystalline polymer, it shows a single broad peak at $2\theta = 20^\circ$ which is attributed to the hydrogen bond interactions between the alkyl group of PVA [39]. The XRD pattern of Zeolite 4A shows multiple sharp peaks indicating its highly crystalline nature. **Fig. 4** shows the XRD patterns of PVA/PEDOT: PSS/Zeolite 4A nanocomposites. After the incorporation of Zeolite 4A into

PEDOT: PSS/PVA blend matrix sharp peaks were observed which resulted in the modifications of the polymer structure.

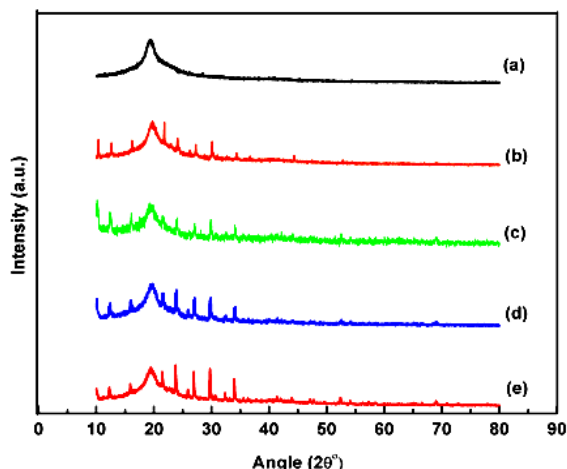


Fig. 4. XRD spectra of PEDOT: PSS/PVA/Zelite 4A nanocomposites films (a) PEDOT: PSS/PVA blend (b) 5 wt % Zeolite 4A (c) 10 wt % Zeolite 4A (d) 15 wt % Zeolite 4A (e) 20 wt % Zeolite 4A.

The XRD pattern of nanocomposites showed various diffraction peaks at $2\theta = 10.4^\circ$, 12.8° , 16.5° , 21.6° , 24° , 26.2° , 27° , 30° and 34.3° which are the characteristics reflections of α phase of Zeolite 4A and can be indexed into (220), (222), (420), (440), (600), (622), (640) and (664) respectively. The presence of these XRD peaks in the nanocomposites samples confirms the presence of Zeolite 4A nanoparticles in the nanocomposites. The crystalline nature of these nanocomposites shows considerable changes which are due to hydrogen bonding interaction between the hydroxyl groups of PVA and alkyl group in Zeolite 4A. Thus, from XRD analysis, it was observed that the dispersion of Zeolite 4A is uniform throughout the polymer matrix.

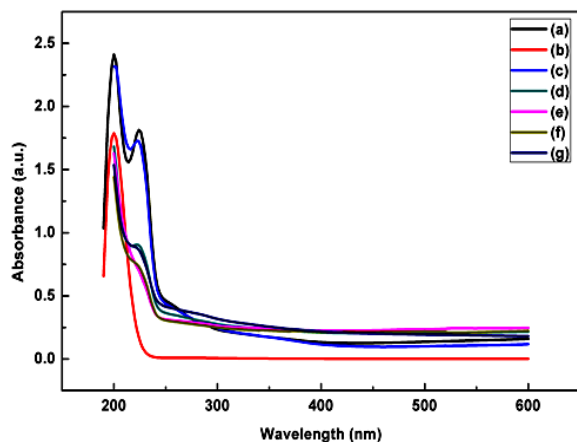


Fig. 5. UV-vis spectra of PEDOT: PSS/PVA/Zelite 4A nanocomposites (a) PEDOT: PSS (b) PVA (c) PEDOT: PSS/PVA blend (d) 5 wt % Zeolite 4A (e) 10 wt % Zeolite 4A (f) 15 wt % Zeolite 4A (g) 20 wt % Zeolite 4A.

UV-vis spectroscopy

UV-vis absorption spectroscopy is commonly used to study the interaction between electrons and radiation [40]. The

UV-vis absorbance spectra of PEDOT: PSS, neat PVA, PEDOT: PSS/PVA blend and PEDOT: PSS/PVA/Zelite 4A dispersion is shown in **Fig. 5(a-g)**. The UV-vis absorbance spectra of PEDOT: PSS has shown a single absorption peak at 225 nm which can be attributed to the π - π^* transitions of benzene rings of PSS [41]. The UV-vis spectra of neat PVA has shown a UV absorbance peaks at 200 nm. The absorption spectra of PEDOT: PSS/PVA blend shows two absorbance bands at 200 nm and 230 nm which are characteristics bands of both PEDOT: PSS and PVA. PEDOT: PSS/PVA/Zelite 4A dispersion with different loading of Zeolite 4A also shows two distinct absorption bands in the range of 190-230 nm. These results indicate that Zeolite 4A was homogeneously dispersed in the polymer matrix.

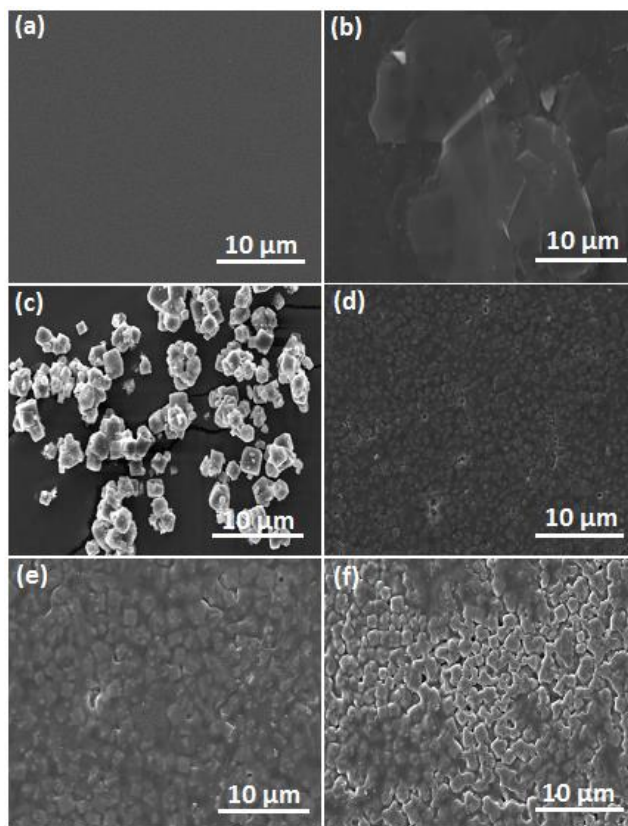


Fig. 6. SEM micrographs of PEDOT: PSS/PVA/Zelite 4A nanocomposites (a) Pure PVA film (b) PEDOT: PSS/PVA blend (c) Zeolite 4A nanoparticles (d) 5 wt % Zeolite 4A (e) 10 wt % Zeolite 4A (f) 20 wt % Zeolite 4A.

Scanning electron microscopy (SEM) studies

Scanning electron microscopy has been used to study the compatibility between various components of the polymer nanocomposites through the detection of phase separation and particle dispersion [42]. The SEM images of PVA and PEDOT: PSS film, Zeolite 4A nanoparticles and PEDOT: PSS/PVA/Zelite 4A nanocomposites are shown in **Fig. 6(a-f)**. Pure PVA film shows smooth surface while PEDOT: PSS/PVA blend film shows rough surface compare to neat PVA. This indicates a good interfacial interaction between the PVA and PEDOT: PSS. The SEM micrographs of Zeolite 4A nanoparticles show cubic shaped structure while Zeolite 4A incorporated PEDOT: PSS/PVA

blend matrix shows microporous structure. It was observed that increasing the Zeolite 4A loadings has changed the surface morphology of PEDOT: PSS/PVA/Zeolite 4A nanocomposites significantly. The SEM micrographs of nanocomposites indicate that Zeolite nanoparticles have uniformly dispersed throughout the polymer matrix.

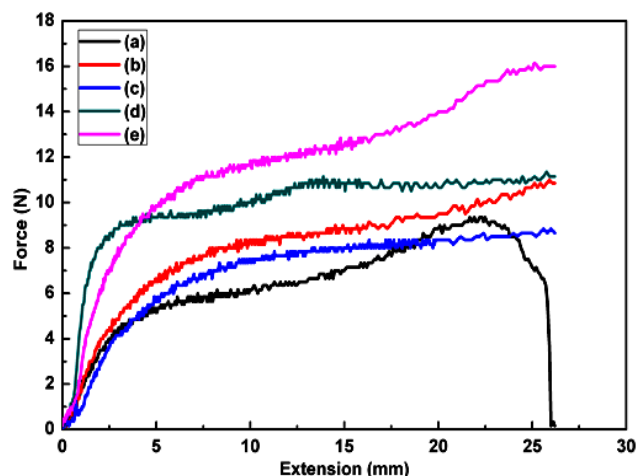


Fig. 7. Force versus extension plots of PEDOT: PSS/PVA/Zeolite 4A nanocomposites (a) PEDOT: PSS/PVA blend (b) 5 wt% Zeolite 4A (c) 10 wt% Zeolite 4A (d) 15 wt% Zeolite 4A (e) 20 wt% Zeolite 4A.

Mechanical properties

The mechanical properties are most important for the selection of polymer material for suitable applications [43]. **Fig. 7(a-e)** shows the force vs. extension plot of PEDOT: PSS/PVA/Zeolite 4A nanocomposites. It can be seen that the mechanical properties of nanocomposites have changed significantly due to the incorporation of Zeolite 4A nanoparticles. The significant change in the mechanical behavior is due to the homogeneous dispersion of Zeolite 4A nanoparticles into the polymer matrix and interfacial interactions between them. It is very much essential to achieve an efficient level of stress transfer between nanoparticles and the polymer matrix in order to enhance the mechanical properties of nanocomposites [44]. Thus, good interfacial adhesion between Zeolite 4A nanoparticles and PEDOT: PSS/PVA blend matrix and the homogeneous dispersion of Zeolite 4A nanoparticles into the polymer blend matrix have resulted in the enhancement of mechanical properties of nanocomposites [2].

Dielectric studies

The dielectric properties of polymer nanocomposites can be greatly improved as compared to neat polymers, by selecting a suitable combination of polymer matrix and nanoparticles. The inorganic nanoparticles can be introduced into the polymer matrix to form polymer nanocomposites of good dielectric behavior and high energy density [1, 2]. Polymer nanocomposites with high dielectric constant have various applications in energy storage capacitors etc. In the present study, the dielectric properties of PEDOT: PSS/PVA/Zeolite 4A nanocomposite films were investigated in the broadband frequency ranging from 50 Hz to 20 MHz and the temperature ranging from

40 – 150 °C. **Fig. 8(a-e)** shows dielectric constant plots of PEDOT: PSS/PVA blend and PEDOT: PSS/PVA/Zeolite 4A nanocomposite films with different wt% of Zeolite 4A loading.

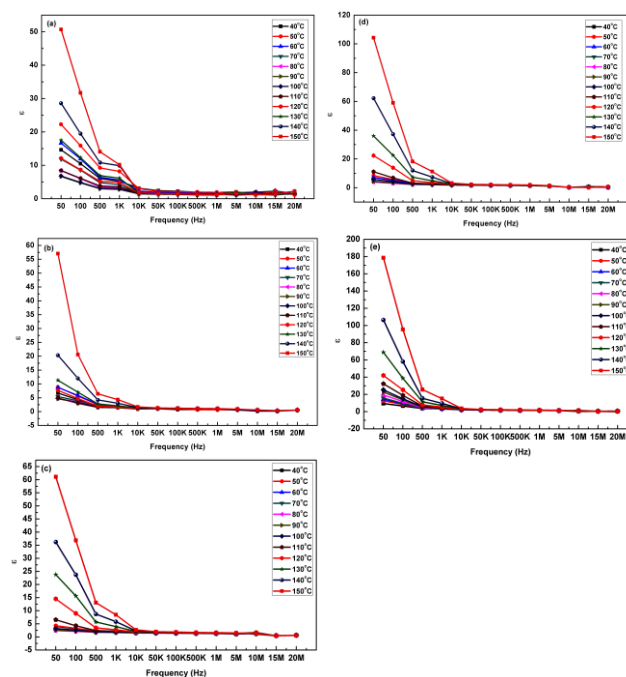


Fig. 8. (a) Dielectric constants of PEDOT: PSS/PVA blend film as a function of frequency at various temperatures, (b) Dielectric constants of PEDOT: PSS/PVA/Zeolite 4A nanocomposite film with 5 wt % Zeolite 4A nanoparticle as a function of frequency at various temperatures, (c) Dielectric constants of PEDOT: PSS/PVA/Zeolite 4A nanocomposite film with 10 wt % Zeolite 4A nanoparticle as a function of frequency at various temperatures, (d) Dielectric constants of PEDOT: PSS/PVA/Zeolite 4A nanocomposite film with 15 wt % Zeolite 4A nanoparticle as a function of frequency at various temperatures, (e) Dielectric constants of PEDOT: PSS/PVA/Zeolite 4A nanocomposite film with 20 wt % Zeolite 4A nanoparticle as a function of frequency at various temperatures.

The maximum value of dielectric constant for PEDOT: PSS/PVA blend film was found to be ($\epsilon = 50.71$, 50 Hz, 150°C) and the maximum value of dielectric constant for PEDOT: PSS/PVA/ Zeolite 4A nanocomposites film with 20 wt % Zeolite 4A loading was found to be ($\epsilon = 178.61$, 50 Hz, 150°C). This indicates that the incorporation of Zeolite 4A into PEDOT: PSS/PVA blend matrix has resulted in the enhancement of dielectric constant of nanocomposites. In general, the dielectric properties of nanocomposites always depend on different types of polarizations mainly dipolar, interfacial and electrode polarizations [37]. **Fig. 9(a-e)** shows dielectric loss ($\tan \delta$) plots of PEDOT: PSS/PVA blend and PEDOT: PSS/PVA/Zeolite 4A nanocomposite film with different wt% of Zeolite 4A loadings. The maximum value of dielectric loss ($\tan \delta$) for PEDOT: PSS/PVA blend film was found to be ($\tan \delta = 2.14$, 50 Hz, 150°C) and that for PEDOT: PSS/PVA/ Zeolite 4A nanocomposites film with 20 wt % Zeolite 4A loading was found to be ($\tan \delta = 3.88$, 50 Hz, 150 °C). All the samples showed high values of dielectric constant and the dielectric loss at the lower frequency (**Table 2**) which could be attributed to the strong

contribution of interfacial polarization and free charge motion within the material [25].

Table 2. Comparative dielectric constant and the dielectric loss values of PEDOT: PSS/PVA/Zeolite 4A nanocomposites.

Zeolite 4A (wt %)	Dielectric Constant (ϵ)	Dielectric Loss ($\tan\delta$)
0	50.71, 50Hz, 150°C	2.14, 50 Hz, 150°C
5	57.05, 50Hz, 150°C	3.02, 50 Hz, 150°C
10	61.13, 50Hz, 150°C	3.18, 50 Hz, 150°C
15	104.31, 50Hz, 150°C	3.29, 50 Hz, 150°C
20	178.614, 50Hz, 150°C	3.88, 50 Hz, 150°C

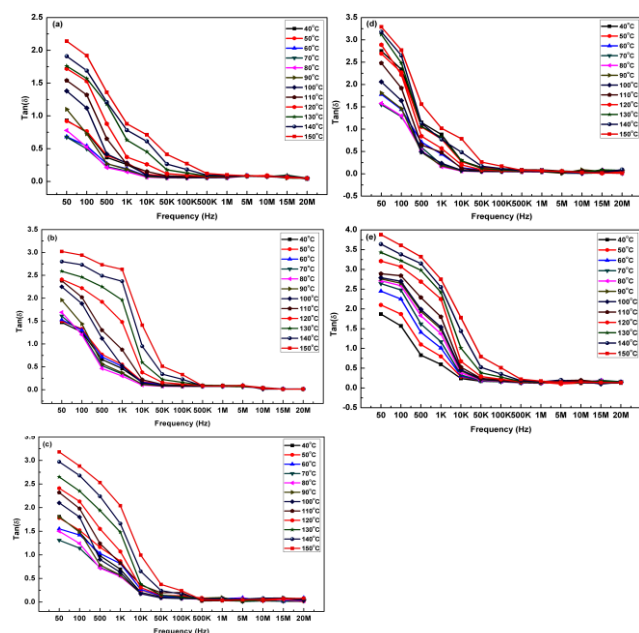


Fig. 9. (a) Dielectric loss ($\tan\delta$) of PEDOT: PSS/PVA blend film as a function of frequency at various temperatures, (b) Dielectric loss ($\tan\delta$) of PEDOT: PSS/PVA/Zeolite 4A nanocomposite film with 5 wt % Zeolite 4A nanoparticle as a function of frequency at various temperatures, (c) Dielectric loss ($\tan\delta$) of PEDOT: PSS/PVA/Zeolite 4A nanocomposite film with 10 wt % Zeolite 4A nanoparticle as a function of frequency at various temperatures, (d) Dielectric loss ($\tan\delta$) of PEDOT: PSS/PVA/Zeolite 4A nanocomposite film with 15 wt % Zeolite 4A nanoparticle as a function of frequency at various temperatures, (e) Dielectric loss ($\tan\delta$) of PEDOT: PSS/PVA/Zeolite 4A nanocomposite film with 20 wt % Zeolite 4A nanoparticle as a function of frequency at various temperatures.

Hence, it is possible to tune the dielectric properties of nanocomposites with desired value of dielectric constant and dielectric loss can be significantly reduced for practical applications. Thus, the significant enhancement in the dielectric constant of nanocomposites makes them a potential candidate for applications in electronic devices such as embedded capacitors.

Conclusion

Zeolite 4A nanoparticles were successfully incorporated into PEDOT: PSS/PVA blend matrix to prepare PEDOT: PSS/PVA/Zeolite 4A nanocomposites using solution casting technique. The Zeolite 4A nanoparticles were well distributed within the polymer matrix without any aggregation. The structural and functional groups present in

PEDOT: PSS/PVA/Zeolite 4A nanocomposites were investigated by FTIR and XRD analysis. From the XRD results, the presence of Zeolite 4A in the nanocomposites was confirmed. FTIR spectroscopy results confirm the different functional groups present in the nanocomposites corresponding to both polymers as well as Zeolite 4A nanoparticle. The UV-vis absorbance results reveal the interaction between the Zeolite 4A nanoparticles and PEDOT: PSS/PVA blend matrix. The morphological study of PEDOT: PSS/PVA/Zeolite 4A nanocomposite confirms the homogeneous dispersion of Zeolite 4A into the PEDOT: PSS/PVA blend matrix leading to the formation of microporous structure. Incorporation of Zeolite 4A nanoparticles in the PEDOT: PSS/PVA blend matrix has resulted in the improvement of the mechanical properties of nanocomposites. In addition, the incorporation of Zeolite 4A into PEDOT: PSS/PVA blend matrix has resulted in the enhancement of dielectric constant of nanocomposites. For example, the dielectric constant for PEDOT: PSS/PVA blend film was found to be ($\epsilon = 50.71$, 50 Hz, 150°C) and that for PEDOT: PSS/PVA/Zeolite 4A nanocomposites film with 20 wt % Zeolite 4A loading was ($\epsilon = 178.61$, 50 Hz, 150°C). The significant enhancement in the dielectric constant of nanocomposites makes them a potential candidate for applications in electronic devices such as embedded capacitors.


Acknowledgements

M. K. Mohanapriya would like to acknowledge the management of VIT University for providing the facilities for XRD and SEM analysis through DST-FIST scheme.

References

- Deshmukh K.; Ahamed M. B.; Deshmukh R.R.; Bhagat, P. R.; Khadheer Pasha S. K. K.; Bhagat A.; Shirbhate R.; Telare F.; Lakhani C. *Polym. Plast. Tech.* **2016**, 55, 231.
DOI: [10.1080/03602559.2015.1055499](https://doi.org/10.1080/03602559.2015.1055499)
- Shukla SK, Deshpande SR, Shukla SK, Tiwari A, *Talanta*, **2012**, 99, 283-287.
DOI: [10.1016/j.talanta.2012.05.052](https://doi.org/10.1016/j.talanta.2012.05.052)
- Ahmad, J.; Deshmukh, K.; Hagg, M.B.; *Int. J. Polym. Anal. Charact.* **2013**, 18, 287.
DOI: [10.1080/1023666X.2013.767080](https://doi.org/10.1080/1023666X.2013.767080)
- Ahmad, J.; Deshmukh K.; Habib M.; Hagg M.B. *Arab J. Sci. Eng.* **2014**, 39, 6805.
DOI: [10.1007/s13369-014-1287-0](https://doi.org/10.1007/s13369-014-1287-0)
- Mahajan R.; Burns R.; Schaeffer M.; Koros, W.J. *J. Appl. Polym. Sci.* **2002**, 86, 881.
DOI: [10.1002/app.10998](https://doi.org/10.1002/app.10998)
- Mahajan R.; Koros, W.J.; *Ind. Eng. Chem. Res.* **2000**, 39, 2692.
DOI: [10.1021/ie990799r](https://doi.org/10.1021/ie990799r)
- Bottino, A.; Capannelli, G.; Asti, V.D.; Piaggio, P.; *Sep. Purif. Technol.* **2001**, 22, 269.
DOI: [10.1016/S1383-5866\(00\)00127-1](https://doi.org/10.1016/S1383-5866(00)00127-1)
- Yang, Y.; Wang, P.; Zheng Q.; *J. Polym. Sci. Part B: Polym. Phys.* **2006**, 44, 879.
DOI: [10.1002/polb.20715](https://doi.org/10.1002/polb.20715)
- Jian, P.; Yahui H.; Yang, W.; Linlin L.; *J. Membr. Sci.* **2006**, 284, 9.
DOI: [10.1016/j.memsci.2006.07.052](https://doi.org/10.1016/j.memsci.2006.07.052)
- Yan, L.; Li, Y.S.; Xiang, C.B.; Xianda, S.; *J. Membr. Sci.* **2006**, 276, 162.
DOI: [10.1016/j.memsci.2005.09.044](https://doi.org/10.1016/j.memsci.2005.09.044)
- Xu, Z. L.; Yu, L.Y.; Han, L.F.; *Frontiers Chem. Eng. China*. **2009**, 3, 318.
DOI: [10.1007/s11705-009-0199-0](https://doi.org/10.1007/s11705-009-0199-0)
- Groendaal L.B.; Jonas F.; Freitag D.; Pielartzik H.; Reynolds J. R. *Adv. Mater.* **2000**, 12, 481.
DOI: [10.1002/\(SICI\)1521-4095\(200004\)12:7<481::AID-ADMA481>3.0.CO;2-C](https://doi.org/10.1002/(SICI)1521-4095(200004)12:7<481::AID-ADMA481>3.0.CO;2-C)

13. Kim, J.Y.; Chung, I.J.; Kim, Y.C.; Yu, J. W.; *J. Korean Phys. Soc.* **2004**, *45*, 231.
DOI: [10.3938/jkps.45.231](https://doi.org/10.3938/jkps.45.231)
14. Ouyang, J.; Chu, C.W.; Xu, Q.; Yang, Y.; *Adv. Funct. Mater.* **2008**, *18*, 865.
DOI: [10.1002/adfm.200700796](https://doi.org/10.1002/adfm.200700796)
15. Liu, F.J.; *J. Power Sources*, **2008**, *182*, 383.
DOI: [10.1016/j.jpowsour.2008.04.008](https://doi.org/10.1016/j.jpowsour.2008.04.008)
16. Hong, W.; Yuxi, X.; Gewu, L.; Chun, L.; Gaoquan, S.; *Electrochem. Comm.* **2008**, *10*, 1555.
DOI: [10.1016/j.elecom.2008.08.007](https://doi.org/10.1016/j.elecom.2008.08.007)
17. Arais A.C.; Granstrom M.; Thomas D.S.; Petritsch K.; Friend R.H. *Phys. Rev. B.* **1999**, *60*, 1854.
DOI: [10.1103/PhysRevB.60.1854](https://doi.org/10.1103/PhysRevB.60.1854)
18. Jonas F.; Hevwang, G.; *Electrochim Acta* **1994**, *39*, 1345.
DOI: [10.1016/0013-4686\(94\)E0057-7](https://doi.org/10.1016/0013-4686(94)E0057-7)
19. Jonas F.; Kraft W.; Muys B. *Macromol. Symp.* **1995**, *100*, 169.
DOI: [10.1002/masy.19951000128](https://doi.org/10.1002/masy.19951000128)
20. Heur, H. W.; Wehrmann R.; Kirchmeyer S.; *Adv. Funct. Mater.* **2002**, *12*, 89.
DOI: [10.1002/1616-3028\(20020201\)12:2<89::AID-ADFM89>3.0.CO;2-1](https://doi.org/10.1002/1616-3028(20020201)12:2<89::AID-ADFM89>3.0.CO;2-1)
21. Woo, H.S.; Kim, Y.B.; Czerw R.; Carrol D.L.; Ballato J.; Ajayan P.M. *J. Korean Phys. Soc.* **2004**, *45*, 507.
DOI: [10.3938/jkps.45.50](https://doi.org/10.3938/jkps.45.50)
22. Pawde, S.M.; Deshmukh, K.; Parab, S. *J. Appl. Polym. Sci.* **2008**, *109*, 1328.
DOI: [10.1002/app.28096](https://doi.org/10.1002/app.28096)
23. Pawde, S.M.; Deshmukh, K. *J. Appl. Polym. Sci.* **2008**, *109*, 3431.
DOI: [10.1002/app.28454](https://doi.org/10.1002/app.28454)
24. Deshmukh, K.; Ahmad, J.; Hagg, M.B. *Ionics*, **2014**, *20*, 957.
DOI: [10.1007/s11581-013-1062-3](https://doi.org/10.1007/s11581-013-1062-3)
25. Deshmukh, K.; Ahamed, M.B.; Pasha, S.K.K.; Deshmukh, R.R.; Bhagat, P.R. *RSC Advances* **2015**, *5*, 61933.
DOI: [10.1039/c5ra11242g](https://doi.org/10.1039/c5ra11242g)
26. Zhu, M.H.; Qian, J. W.; Zhao, Q. A.; An, Q.F.; Li, J. *J. Membr. Sci.* **2010**, *361*, 182.
DOI: [10.1016/j.memsci.2010.05.058](https://doi.org/10.1016/j.memsci.2010.05.058)
27. Wang, X.Q.; Yucel, T.; Lu, Q.; Hu, X.; Kaplan, D. L. *Biomaterials*, **2010**, *31*, 1025.
DOI: [10.1016/j.biomaterials.2009.11.002](https://doi.org/10.1016/j.biomaterials.2009.11.002)
28. Cavalieri, F.; Chiessi, Villa, R.; Vigano, I.; Zaffaroni, N.; Telling, M.F.; Paradossi, G. *Biomacromolecules* **2008**, *9*, 1967.
DOI: [10.1021/bm800225v](https://doi.org/10.1021/bm800225v)
29. Abdelrazek, E.M.; Elashmawi, I. S.; Labeeb, S. *Physica B*, **2010**, *405*, 2021.
DOI: [10.1021/bm800225v](https://doi.org/10.1021/bm800225v)
30. Jeong, S. K.; Jo, Y.K.; Jo, N. J. *Electrochim. Acta*, **2006**, *52*, 1549.
DOI: [10.1016/j.electacta.2006.02.061](https://doi.org/10.1016/j.electacta.2006.02.061)
31. Fritz, L.; Hofmann, D. *Polymer*, **1997**, *38*, 1035.
DOI: [10.1016/S0032-3861\(96\)00600-3](https://doi.org/10.1016/S0032-3861(96)00600-3)
32. Ahmad, J.; Hagg, M.B. *Sep. Pur. Tech.* **2013**, *115*, 190.
DOI: [10.1016/j.seppur.2013.04.049](https://doi.org/10.1016/j.seppur.2013.04.049)
33. Ahmad, J.; Hagg, M.B. *Sep. Pur. Tech.* **2013**, *115*, 163.
DOI: [10.1016/j.seppur.2013.04.050](https://doi.org/10.1016/j.seppur.2013.04.050)
34. Gur, T.M.; *J. Membr. Sci.*, **1994**, *93*, 283.
DOI: [10.1016/0376-7388\(94\)00102-2](https://doi.org/10.1016/0376-7388(94)00102-2)
35. Shakarova, D.; Ojuva, A.; Bergstrom, L.; Akhtar, F.; *Materials*, **2014**, *7*, 5507.
DOI: [10.3390/ma7085507](https://doi.org/10.3390/ma7085507)
36. Zamani, F.; Rezapour, M.; Kianpour, S.; *Bull. Korean Chem. Soc.* **2013**, *34*, 2367.
DOI: [10.5012/bkcs.2013.34.8.2367](https://doi.org/10.5012/bkcs.2013.34.8.2367)
37. Deshmukh, K.; Ahamed, M. B.; R.R. Deshmukh, Pasha, S.K.K. Sadasivuni, K.K. Ponnammam, D.; Chidambaram, K.; *Euro. Polym. J.* **2016**, *76*, 14.
DOI: [10.1016/j.eurpolymj.2016.01.022](https://doi.org/10.1016/j.eurpolymj.2016.01.022)
38. Rondon, W.; Freire, D.; Benzo, Z.; Sifontes, AB; Gonzalez, Y; Valero, M; *Amer. J. Anal. Chem.* **2013**, *4*, 584.
DOI: [10.4236/ajac.2013.410069](https://doi.org/10.4236/ajac.2013.410069)
39. Ahmad, J; Hagg, M.B; *J. Membr. Sci.*, **2013**, *427*, 73.
DOI: [10.1016/j.memsci.2012.09.036](https://doi.org/10.1016/j.memsci.2012.09.036)
40. Zidan, H.M; *Polym. Test*, **1999**, *18*, 449.
DOI: [10.1016/S0142-9418\(98\)00049-X](https://doi.org/10.1016/S0142-9418(98)00049-X)
41. Pettersson L.A.A.; Ghosh, S.; Inganas, O. *Org. Electron.* **2002**, *3*, 143.
DOI: [10.1016/S1566-1199\(02\)00051-4](https://doi.org/10.1016/S1566-1199(02)00051-4)
42. Zou, P.; Feng, H.; Xu, Z.; Zhang, L.; Zhang, Y.; Xia, W.; Zhang, W.; *Chem. Cent. J.*, **2013**, *7*, 39.
DOI: [10.1186/1752-153X-7-39](https://doi.org/10.1186/1752-153X-7-39)
43. Prashantha K, Soulestin J, Lacrampe M.F., Claes M, Dupin G, Krawczak P, *Exp. Polym. Lett.* **2008**, *2*, 735.
DOI: [10.3144/expresspolymlett.2008.87](https://doi.org/10.3144/expresspolymlett.2008.87)
44. Pawde, S. M.; Deshmukh, K. *J. Appl. Polym. Sci.* **2009**, *114*, 2169.
DOI: [10.1002/app.30641](https://doi.org/10.1002/app.30641)



Advanced Materials Letters

Volume 1, December 2015


Copyright © 2016 VBRI Press AB, Sweden

A Monthly Journal

Publish your article in this journal

Advanced Materials Letters is an official international journal of International Association of Advanced Materials (IAAM, www.iaamonline.org) published monthly by VBRI Press AB from Sweden. The journal is intended to provide high-quality peer-review articles in the fascinating field of materials science and technology particularly in the area of structure, synthesis and processing, characterisation, advanced-state properties and applications of materials. All published articles are indexed in various databases and are available download for free. The manuscript management system is completely electronic and has fast and fair peer-review process. The journal includes review article, research article, notes, letter to editor and short communications.

www.vbripress.com/aml



VBRI Press
Commitment to Excellence